Pan-cancer analysis of the oncogenic role of SRY-related high-mobility group box protein B5 in human tumors

YAJUN TONG[1*], HUINI DA[2*], KEWEI TANG[1], QIANG ZHOU[1], SONGLIAN LIU[1], LEILAN YIN[1], LING LONG[1], SITE BAI[1], LUDI OU[1] and QINGHUA YIN[1]

[1]Department of Oncology, Yueyang Central Hospital, Yueyang, Hunan 414000, P.R. China; [2]Department of Urology, Yueyang Central Hospital, Yueyang, Hunan 414000, P.R. China

Received June 19, 2025; Accepted November 14, 2025

DOI: 10.3892/etm.2025.13027

Abstract. SRY-related high-mobility group protein B5 (SOX5) functions as an oncogene in diverse human malignancies, contributing to tumor progression, metastasis and therapy resistance across various cancer types. In light of this, a pan-cancer analysis was performed in the present study to investigate the oncogenic function of SOX5 in various human malignancies. SOX5 mRNA expression levels were compared between normal and malignant tissues using The Cancer Genome Atlas database and diagnostic effectiveness was evaluated using receiver operating characteristic curve analysis. Kaplan-Meier survival analysis was performed to investigate the association between SOX5 expression and overall survival, disease-specific survival, disease-free interval and progression-free interval. The influence of SOX5 on immune infiltration and immunological scores in the tumor microenvironment was assessed utilizing Estimation of Stromal and Immune Cells in Malignant Tumor Tissues Using Expression Data, Cell-Type Identification by Estimating Relative Subsets of RNA Transcripts and single-sample Gene Set Enrichment Analysis methodologies, in conjunction with its relationship to drug sensitivity and genetic modifications. SOX5 exhibited tissue-specific dysregulation, being markedly downregulated in carcinomas such as lung adenocarcinoma (LUAD), lung squamous cell carcinoma and breast cancer, while increased in testicular germ cell tumor and non-small cell lung cancer (NSCLC) cell lines. It demonstrated notable diagnostic potential, with good performance in LUAD (area under the curve=0.916). The prognostic relevance of SOX5 was contingent upon context as lower expression conferred protection in specific malignancies; however, it was associated with worse outcomes in others, such as low-grade glioma and pancreatic adenocarcinoma. Increased SOX5 expression was associated with an immunosuppressive milieu marked by a rise in regulatory T cells, a decline in cytotoxic T cells and the activation of immunological checkpoints including programmed death-ligand 1 and cytotoxic T lymphocyte associated protein 4. Moreover, SOX5 was associated with genomic instability, susceptibility to medicines such as azacitidine and distinct mutation patterns. SOX5 suppression in NSCLC cells *in vitro* impeded proliferation, migration and invasion. These findings collectively emphasize the key function of SOX5 in tumor biology and highlight its potential as a biomarker for cancer diagnosis, prognosis and therapeutic targeting.

Correspondence to: Professor Qinghua Yin, Department of Oncology, Yueyang Central Hospital, 39 Dongmaoling Road, Yueyanglou, Yueyang, Hunan 414000, P.R. China
E-mail: tsinghuayin@hotmail.com

*Contributed equally

Key words: SOX5, human tumors, carcinogenesis, pan-cancer analysis

Introduction

SRY-related high-mobility group box protein B5 (SOX5), a member of the SRY-related HMG-box gene family, has gained interest for its functions in developmental biology and disease pathogenesis (1-5). In tumor biology, abnormal SOX5 expression and activity is associated with the advancement of a number of human malignancies, including hepatocellular carcinoma [promoting epithelial-mesencymal transition (EMT) and invasion], bladder cancer (modulating migration and therapy resistance), prostate cancer (driving metastasis via EMT), ovarian cancer (regulating glycolysis and proliferation), gastric cancer (enhancing proliferation and migration), tongue carcinoma (facilitating tumorigenesis) and esophageal squamous cell carcinoma (where its downregulation is associated with a poor prognosis) (6-8). While SOX5 may have tumor-suppressive characteristics in some tissues, its upregulation in numerous malignancies is acknowledged as a notable contributor to tumor growth, rendering it a key subject within cancer research.

The protein encoded by SOX5 is part of the high mobility group of proteins, which modulate transcription through DNA binding and are key in cell differentiation. In typical physiological conditions, SOX5 regulates collagen synthesis, neural development and cartilage creation. In cancer, the function of SOX5 is altered, potentially facilitating tumor initiation and progression by regulating the cell cycle and promoting malignant behaviors (such as inducing EMT, enhancing cell

migration and invasion, maintaining cancer stem cell properties) or enabling immune evasion (9-12).

Altered SOX5 expression has been documented in a number of malignancies, including lung, breast, gastric cancers and melanoma (13,14). In lung adenocarcinoma (LUAD), increased SOX5 expression is associated with adverse prognosis, including reduced survival and enhanced recurrence rates. This modified expression indicates that SOX5 may enhance tumor cell proliferation and survival by activating downstream signaling pathways, such as Wnt/β-catenin and PI3K/AKT. In addition to its intrinsic effects on tumor cells, SOX5 also affects the tumor microenvironment (TME). It can regulate the activity of tumor-associated fibroblasts, thereby influencing immunological responses and facilitating immune evasion (15-17). Additionally, SOX5 has been associated with the regulation of tumor angiogenesis, highlighting its complex involvement in cancer advancement.

Understanding the varied expression patterns and roles of SOX5 across different tumor types is key for the advancement of novel cancer therapeutics. Consequently, the aims of the present study are threefold: i) To delineate the molecular regulatory network of SOX5; ii) to characterize its distinct involvement in carcinogenesis; and iii) to explore methodologies for improving therapeutic efficacy through the targeting of SOX5-associated pathways. Pan-cancer analysis provides a thorough method to elucidate the role of SOX5 role in tumorigenesis, establishing a theoretical basis and prospective targets for forthcoming clinical therapies.

Materials and methods

Data processing. Within the present study, data from The Cancer Genome Atlas (TCGA; https://portal.gdc.cancer.gov/) was utilized. TCGA is a large-scale cancer genome project jointly funded and managed by the National Cancer Institute and the National Human Genome Research Institute to advance the scientific understanding of cancer. Specifically, RNA-sequencing data (fragments per kilobase format) and clinical annotations from TCGA Pan-Cancer Atlas (version 2018) were obtained through the University of California, Santa Cruz Xena browser (https://xena.ucsc.edu/). Normalization and batch correction were performed using the ComBat algorithm from the 'sva' R package (version 4.3.1) (18) to mitigate technical variations across sequencing centers. Samples with incomplete clinical metadata or low sequencing quality (read count <10 million) were excluded.

For validation, Gene Expression Omnibus (GEO; https://www.ncbi.nlm.nih.gov/geo/) datasets (GSE30219, GSE31210 and GSE50081) (19-21) were retrieved using the 'GEOquery' R package (22). Probes were annotated to gene symbols based on platform-specific annotation files (such as the platform name 'GPL570' for the array name 'Affymetrix Human Genome-U133 Plus 2.0'). For genes mapped by multiple probes, the duplicates were collapsed by selecting the single probe with the maximum mean expression value across all samples for that gene. Additionally, the 'TCGAbiolinks' R package (23) was employed to download and access TCGA data, facilitating the integration and bioinformatics analysis of numerous data types.

Expression of SOX5 gene in a number of cancers. Differential SOX5 expression across tumor and corresponding normal tissues in TCGA was examined through use of the 'TCGAplot' R package (version 1.0) (24). For cancers lacking normal tissue data in TCGA [including diffuse large B cell lymphoma (DLBC) and mesothelioma (MESO)], GEO datasets (GSE12453 and GSE51024) (25,26) were supplemented. Normalized $\log_2$-transformed expression values from both sources were compared using Wilcoxon rank-sum tests. This analysis provided SOX5 expression profiles in normal and tumor tissues for cancers including DLBC, low-grade glioma, MESO, ovarian serous cystadenocarcinoma, testicular germ cell tumor (TGCT), uterine carcinosarcoma and uveal melanoma.

Diagnosis and prognosis analysis. Using TCGA data, the diagnostic potential of SOX5 was assessed by generating receiver-operating characteristic (ROC) curves with the 'pROC' R package (27). An area under the curve (AUC) value of 0.5-0.7 indicated a low diagnostic value, 0.7-0.9 indicated a moderate value and >0.9 indicated a high diagnostic value. Prognostic associations of SOX5 expression with overall survival (OS), disease-specific survival (DSS), disease-free interval (DFI) and progression-free interval (PFI) were evaluated using the SangerBox database (version 3.0; http://sangerbox.com/). Statistical significance was determined using multiple-testing correction (the Benjamini-Hochberg method) (28). Patients were stratified by median SOX5 expression and multivariate Cox regression adjusted for age, stage and sex was applied where appropriate.

Correlation analysis of immune infiltration. Immune infiltration in the TME was assessed by calculating Stromal Score, Immune Score and Estimation of Stromal and Immune Cells in Malignant Tumor Tissues Using Expression Data (ESTIMATE) Score using the 'ESTIMATE' R package (29). The cancer immunity cycle was analyzed using the Tumor Immune Estimation Resource 2.0 web tool (http://timer.cistrome.org/) to evaluate correlations between SOX5 expression and immune activation steps such as T cell recruitment and antigen presentation. Immune cell fractions were estimated using Cell-Type Identification by Estimating Relative Subsets of RNA Transcripts (CIBERSORT version 1.04) (30) deconvolution and single-sample Gene Set Enrichment Analysis (ssGSEA) through the Gene Set Variation ('GSVA') R package (31) quantified immune cell enrichment. Associations between SOX5 expression and microsatellite instability (MSI), tumor mutational burden (TMB) and immune checkpoint proteins across tumors were analyzed in SangerBox (http://sangerbox.com/) using Pearson correlation tests.

Drug sensitivity analysis. Drug sensitivity data from the Genomics of Drug Sensitivity in Cancer 2 database (version Release 8.5) (https://www.cancerrxgene.org/) were processed using the 'oncoPredict' R package (version 0.2) (32). IC_{50} values were estimated through ridge regression and normalized to Z-scores. Drugs with a Z-score >2 were considered to be significantly associated with SOX5 expression.

Analysis of tumor mutation patterns. The cBioPortal database (https://www.cbioportal.org/) was used to explore associations between SOX5 expression and tumor mutation patterns. Somatic mutations and copy-number alterations were retrieved from cBioPortal (TCGA Pan-Cancer Atlas; version 2018). Patients were divided into high and low SOX5 expression groups (top/bottom 25%; high SOX5, n=250; low SOX5, n=261). Mutational signatures were visualized using the 'Maftools' package (version 2.6.05) (33), enabling comprehensive analysis of somatic mutation patterns in TCGA-LUAD cohort.

Functional enrichment analysis. Co-expression networks were constructed using LinkedOmics (www.linkedomics.org; TCGA_LUAD cohort; HiSeq platform) with Pearson correlation [r>0.3; false discovery rate (FDR) <0.05] to identify genes co-expressed with SOX5. GSEA of Molecular Signatures Database Hallmark and Kyoto Encyclopedia of Genes and Genomes (KEGG) gene sets, as well as GSVA of Gene Ontology terms were performed to explore associated biological functions and pathways. Analyses were performed with 1,000 permutations and results with FDR-adjusted P<0.05 were considered significant.

Cell culture. Human non-small cell lung cancer (NSCLC) cell lines A549 and H1299, as well as the normal human bronchial epithelial cell line BEAS-2B, were obtained from the Cell Bank of the Chinese Academy of Sciences (Shanghai Institute of Biochemistry and Cell Biology). H1299, A549 and BEAS-2B normal lung epithelial cells were cultured in DMEM supplemented with 10% FBS (Gibco; Thermo Fisher Scientific, Inc.) at 37˚C in a humidified incubator with 5% CO_2. Cells were digested every 48 h with 0.25% trypsin-EDTA (Gibco; Thermo Fisher Scientific, Inc.) and passaged at a 1:3 ratio. Experiments utilized cells between passages 5-20.

Cell transfection. For SOX5 knockdown, A549 cells were transfected with 50 nM of a SOX5-targeting siRNA (sense, 5'-GGGUCGUGUUCAAUCUUAUU-3' and antisense, 5'-UUAAGAUUGAACACGACCCUU-3'; Shanghai GenePharma Co., Ltd.) or a scrambled control siRNA (sense, 5'-GGCUGGUAGUUGGCAUUUAUU-3' and antisense, 5'-UAAAUGCCAACUACCAGCCUU-3'; Shanghai GenePharma Co., Ltd.) using Lipofectamine™ RNAiMAX (Invitrogen; Thermo Fisher Scientific, Inc.) according to the manufacturer's instructions. Following transfection, cells were incubated at 37˚C in a 5% CO_2 atmosphere for 24 h to allow for efficient knockdown. Experimental groups consisted of the untreated control, scrambled siRNA control and SOX5 knockdown. SOX5 expression was measured after the 24-h incubation period using quantitative PCR (qPCR).

Cell Counting Kit-8 (CCK-8) assay. At 24 h post-transfection, cells were seeded in 96-well plates ($5x10^3$ cells/well) and incubated for 24 h. Furthermore, 10 μl of Cell Counting Kit-8 (CCK-8) solution (Dojindo Molecular Technologies, Inc.) was added to each well and the plates were incubated for 4 h. A total of 150 μl DMSO was added to each well to dissolve the formazan crystals. The absorbance at 490 nm was then measured using a microplate reader (BioTek Synergy HTX; BioTek; Agilent Technologies, Inc.). Cytotoxic activity (%) using optical density (OD) values was calculated as:

$$\text{Cytotoxicity} = \frac{OD_{treatment} - OD_{blank}}{OD_{control} - OD_{blank}} \times 100\%$$

Wound healing assay. Cell migration was evaluated by monitoring wound closure over 24 h. Cells were grown to ~80% confluence in 6-well plates,, scratched with a sterile 200 μl pipette tip, washed with PBS and cultured in serum-free DMEM. Images were captured at 0 and 24 h using the Axiovert 200 microscope (Zeiss GmbH) and analyzed with ImagePro Plus software (version 6.0). Experiments were performed in triplicate.

Transwell invasion assay. After 24 h of transfection, cells ($5x10^4$/well) were seeded into Transwell chambers. The chambers were pre-coated with Matrigel by incubating with a diluted Matrigel solution at 37˚C for 1 h to allow for polymerization. The cells were then plated in serum-free medium. Medium containing 10% FBS was added to the lower chamber. After a 24-h incubation period at 37˚C, non-migrated cells on the upper surface of the membrane were carefully removed with a cotton swab. The invaded cells on the lower surface were fixed with 95% ethanol for 15 min at room temperature and subsequently stained with 0.1% crystal violet for 20 min at room temperature. After washing and air-drying, the cells were imaged in three random fields per chamber at x100 magnification using an inverted light microscope (Olympus Corporation).

Reverse Transcription Quantitative PCR (RT-qPCR). Total RNA was isolated from cultured A549 cells using the TRIzol™ reagent (Invitrogen; Thermo Fisher Scientific, Inc.) according to the manufacturer's protocol. RNA concentration and purity were determined spectrophotometrically. Subsequently, 1 μg of total RNA was reverse-transcribed into cDNA using the PrimeScript™ RT Reagent Kit (Takara Bio Inc.) in strict accordance with the manufacturer's instructions. qPCR was performed using PowerUp™ SYBR™ Green Master Mix (cat. no. A25742; Applied Biosystems) on an Applied Biosystems 7500 Real-Time PCR System. The thermal cycling conditions were as follows: Initial denaturation at 95˚C for 2 min; followed by 40 cycles of denaturation at 95˚C for 15 sec and annealing/extension at 60˚C for 1 min. A melting curve analysis was performed post-amplification to verify reaction specificity. Relative mRNA expression levels were calculated using the $2^{-\Delta\Delta Cq}$ method (34), with GAPDH serving as the internal reference gene for normalization using the following formulae: $\Delta Cq=Cq_{target}-Cq_{GAPDH}$; $\Delta\Delta Cq=\Delta Cq_{reference}-\Delta Cq_{test}$. The primer sequences were as follows: GAPDH forward, 5'-CATCATCCCTGCCTCTACTGG-3' and reverse, 5'-GTGGGTGTCGCTGTTGAAGTC-3'; and SOX5 forward, 5'-CAGATGGAGAGGTAGCCATGG-3 and reverse, 5'-CCATTGTATTGTGCTGAGAAGTG-3'.

Statistical analysis. Statistical analyses were performed using SPSS (version 26.0; IBM Corp.) and R (version 4.3.1). For comparisons between two groups of continuous variables, the unpaired Student's t-test was used for normally distributed data and the unpaired Mann-Whitney U test for non-normally

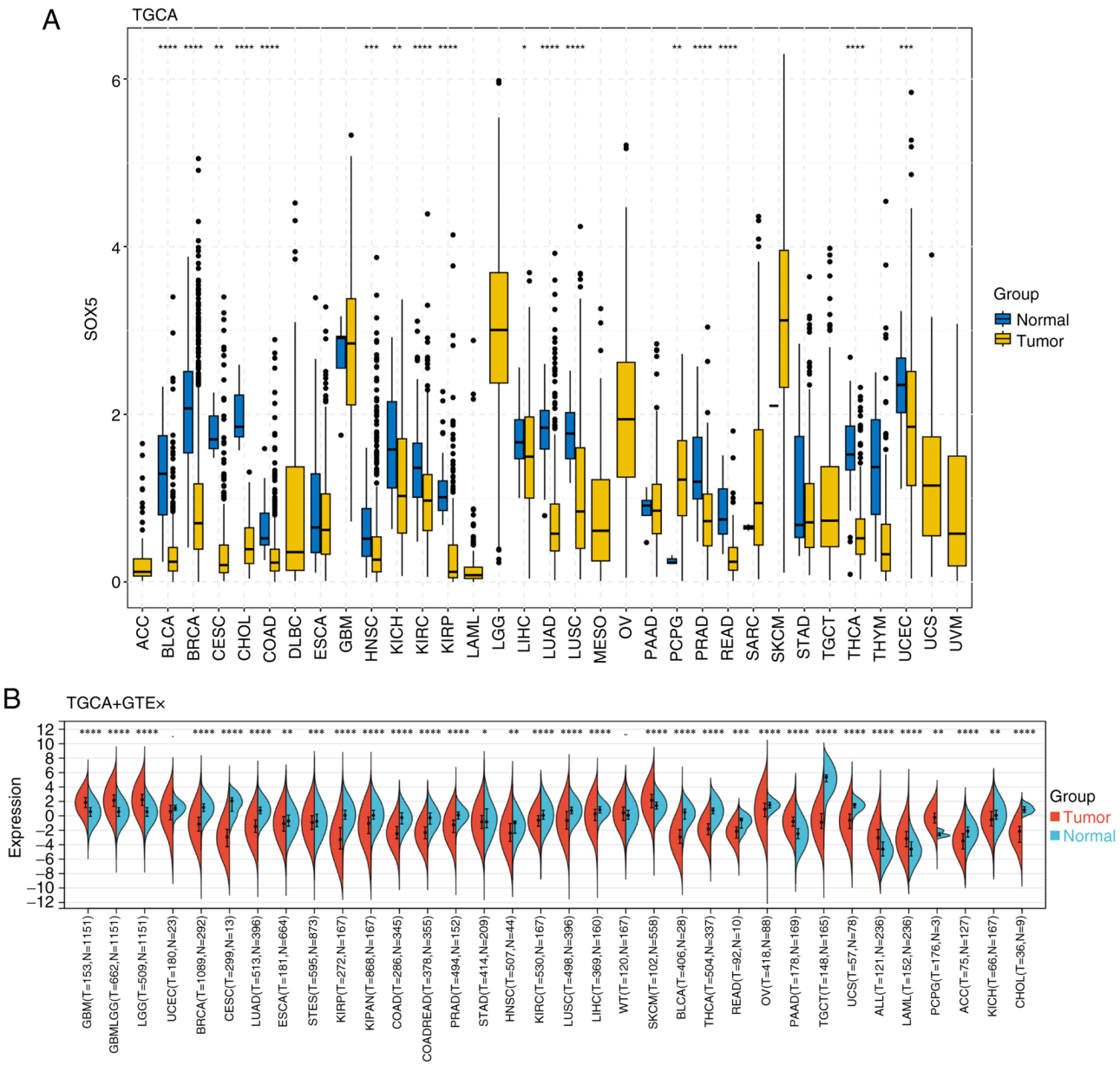

Figure 1. SOX5 expression in human cancers. (A) Boxplots illustrating the mRNA expression levels of SOX5 in normal and cancer tissues using data from TCGA database. Tumor tissues are represented by blue dots and boxes, while normal tissues are represented by orange dots and boxes. (B) Boxplots showing the mRNA expression levels of SOX5 in normal and cancer tissues using data from TCGA database. Tumor tissues are represented by red boxes and normal tissues are represented by blue boxes. *P<0.05; **P<0.01; ***P<0.001; ****P<0.0001. ns, not significant; TCGA, The Cancer Genome Atlas; GTEx, Genotype-Tissue Expression program; SOX5, SRY-related high-mobility group box protein B5.

distributed data. For comparisons among three or more groups, one-way ANOVA (parametric) was applied, followed by Tukey's post hoc test for multiple comparisons. The prognostic value of SOX5 expression was evaluated by univariate Cox regression analysis and Kaplan-Meier survival analysis with the log-rank test. Associations between SOX5 expression and immune-related regulatory factors were assessed using Spearman's rank correlation analysis. A two-sided P-value of <0.05 was considered to indicate a statistically significant difference.

Results

Differential expression of SOX5 in pan-cancer between tumor and normal tissue. Using box plots generated from TCGA database, the expression levels of SOX5 mRNA in tumor and normal tissues were analyzed. As shown in Fig. 1A, SOX5 expression was significantly higher in tumor tissues compared with normal tissues in certain cancer types, such as PCPG (P<0.01). By contrast, in numerous cancers, including LUAD, lung squamous cell carcinoma (LUSC) and breast invasive carcinoma (BRCA), SOX5 mRNA expression was markedly lower in tumor tissues compared with adjacent normal tissues (P<0.05). Fig. 1B further demonstrated this pattern, showing lower SOX5 expression was observed in tumor tissues across the majority of cancers analyzed (P<0.05). Collectively, these results indicate that SOX5 expression is generally reduced in numerous cancer tissues

Predictive value of SOX5 expression for diagnosis and prognosis. Fig. 2 illustrates the diagnostic and prognostic significance of SOX5 across cancers. ROC curve analysis (Fig. 2A) demonstrated good diagnostic performance for head-neck squamous cell carcinoma (AUC=0.953; 95% CI, 0.928-0.978) and LUAD (AUC=0.916; 95% CI, 0.894-0.940), with notable discrimination in 15 additional cancer types (AUC range, 0.508-0.893), all exceeding random chance. Differential expression analysis (Fig. 2B) showed that SOX5 plays an environment-dependent role in tumorigenesis and is progressively dysregulated at various tumor stages. We observed significant differences in six types of tumors, such as STES (Stage I=76; II=201; III=230; IV=57) (P<0.05), STAD (Stage I=58; II=121; III=169; IV=41) (P<0.05), THYM (Stage I=36;II=61;III=14;IV=6) (P<0.05), PAAD (Stage I=21;II=147; III=3;IV=4) (P<0.05), BLCA (Stage II=130;III=140;IV=133) (P<0.05), and KICH (Stage I=21;II=25;III=14;IV=6) (P<0.05). Notably, 78% (18/23) of carcinomas showed marked downregulation of SOX5.

Multivariate survival analysis (Fig. 2C) demonstrated clinically relevant prognostic stratification. Forest plots for OS, DSS, DFI and PFI revealed that elevated SOX5 expression was associated with worse outcomes [hazard ratio (HR) >1; 95% CI, excluding 1] in a number of cancers, while low expression was associated with protective effects (HR <1). These integrated findings suggest that SOX5 is a key dual-purpose biomarker for early cancer detection and precise prognostication.

SOX5 in pan-cancer immune infiltration. The present analysis identified SOX5 as a notable modulator of tumor immune dynamics. Violin plots (Fig. 3A) showed significantly higher SOX5 expression in tumor tissues compared with normal tissues ($P<1x10^{-15}$), while box plots (Fig. 3B) revealed notable inter-cohort heterogeneity. ESTIMATE, CIBERSORT and ssGSEA analyses demonstrated that high SOX5 expression is associated with an activated TME and increased immune scores (P<0.05), particularly in LUAD and UCEC.

Heatmap analysis (Fig. 3C) revealed a negative correlation between SOX5 and cytotoxic T cell infiltration (Pearson r=-0.68; $P<2x10^{-16}$) and a positive correlation between SOX5 and regulatory T cell abundance (r=0.59; $P<5x10^{-9}$), indicating immunosuppressive reprogramming. Radar charts (Fig. 3E and F) further showed that SOX5 expression was inversely correlated with TMB (r=-0.43; P<0.001) and microsatellite instability (r=-0.51; P<0.0001), although subtype-specific variations existed. Correlation networks (Fig. 3D) revealed significant co-expression of SOX5 with immune checkpoint molecules [programmed death-ligand 1 (PD-L1), r=0.62; cytotoxic T-lymphocyte associated protein 4 (CTLA-4), r=0.57; P<0.05], positioning SOX5 as a key regulator of immune evasion and DNA damage response in cancer.

Drug sensitivity analysis. The drug sensitivity screening revealed statistically significant differences in inhibitory potency between the high and low groups for the majority of tested compounds. With the exception of BRD4132, all agents, including azacitidine, betulinic acid, dorsomorphin, etoposide, GW843682X, mitotane, PX-478, S-trityl-L-cysteine, sanguinarine, and selenium, demonstrated markedly enhanced efficacy against the high group (all P<0.001). By contrast, BRD4132 exhibited no significant difference in activity between the two groups (P=0.45). These findings successfully identify a panel of candidate compounds with high potential for selective efficacy against the defined cellular model, providing a substantive basis for further investigation into targeted therapeutic strategies (Fig. 4). Pharmacogenomic profiling of 12 drugs revealed notably distinct IC_{50} distributions between 'SOX5_High' and 'SOX5_Low' cohorts. Wilcoxon rank-sum tests showed significant differences ($P<2.2x10^{-16}$) for 11 compounds, including azacitidine and betulinic acid, with BRD4132 as the only exception (P=0.45). These results highlight SOX5 expression as a potential predictor of therapeutic response, underscoring its value as a precision oncology biomarker.

Tumor mutation pattern analysis. Pan-cancer genomic profiling revealed that SOX5-altered tumors exhibit distinct molecular signatures. Alteration frequency analysis (Fig. 5A) demonstrated prevalent SOX5 mutations and copy-number changes with lineage-specific prevalence, notably in gastric and pancreatic cancers. Detailed characterization (Fig. 5B) showed truncating mutations as the predominant alteration subtype.

Expression stratification (Fig. 5C) revealed that 'SOX5_Low' tumors were associated with transcriptional suppression of cardiac morphogenesis pathways [odds ratio (OR)=0.32; $P<1x10^{-15}$] and upregulation of cell-cycle regulators (OR=3.41; $P<8x10^{-10}$). Waterfall plots (Fig. 5D) demonstrated mutually exclusive alterations between 'SOX5_High' and 'SOX5_Low' groups, with truncating mutations concentrated in 'SOX5_Low_tumors' (P=0.0028) and the analysis demonstrated significant associations between SOX5 expression status and mutations in specific signaling pathways, primarily the PI3K-AKT-mTOR pathway and PD-L1 associated immune regulation (P<0.05). (P<0.05). These findings establish SOX5 loss-of-function as a driver of gene expression changes, especially in LUAD and other cancers with frequent SOX5 variation and amplification.

Functional enrichment analysis. Multi-omics integration revealed SOX5 as a central regulator of cardiac morphogenesis and tumor biology. Pearson correlation analysis (Fig. 6A) showed strong associations (r=1; $P<1x10^{-30}$) with select targets. Z-score clustering (Fig. 6B and C) demonstrated SOX5 co-activation of morphogenetic pathways, such as heart trabecula morphogenesis (Z>3) and cardiac chamber development, alongside suppression of proliferative pathways (cell cycle, Z<-3; small GTPase signaling, Z<-2). KEGG and Hallmark enrichment analyses revealed SOX5 involvement in biological processes including cardiac morphogenesis and angiogenesis, cellular components such as the actin cytoskeleton and molecular functions including actin binding. KEGG analysis (Fig. 6E) implicated SOX5 dysregulation in 'Arrhythmogenic right ventricular cardiomyopathy' pathogenesis ($-\log_{10}P>20$), mediated by altered adhesion molecules, extracellular matrix receptors and metalloproteinases (P<0.05). These findings highlight SOX5 as a key regulator of structural integrity and tumor biology in LUAD.

SOX5 silencing inhibits NSCLC progression in vitro. Functional studies revealed that SOX5 is upregulated in NSCLC cell lines (H1299 and A549) compared with normal bronchial epithelial cells (BEAS-2B; P<0.001; Fig. 7A). SOX5

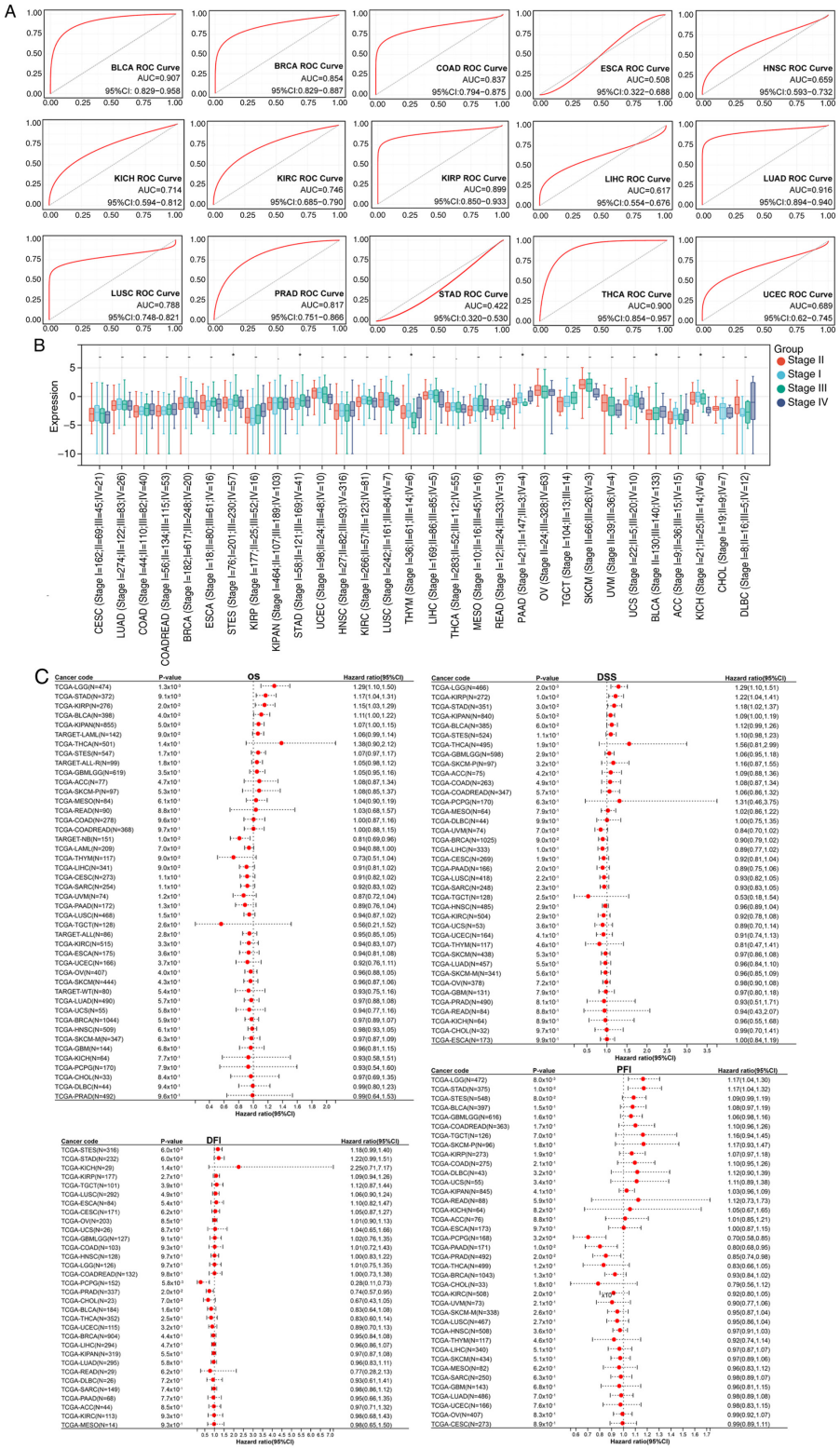

Figure 2. Diagnostic and prognostic value of SOX5 in pan-cancer. (A) ROC curves for diagnosing 15 cancers based on SOX5 expression. (B) Boxplots showing the association between SOX5 expression levels and seven clinical characteristics in 30 cancer types. (C) Circular histogram of OS, DSS, DFI and PFI of SOX5 in 44 types of cancer using Kaplan-Meier analysis. *P<0.05; **P<0.01; ***P<0.001. ns, not significant; ROC, receiver operator characteristic; SOX5, SRY-related high-mobility group box protein B5; OS, overall survival; DSS, disease-specific survival; DFI, disease-free interval; PFI, progression-free interval; BLCA, bladder urothelial carcinoma; BRCA, breast invasive carcinoma; COAD, colon adenocarcinoma; ESCA, esophageal carcinoma; KICH, kidney chromophobe; KIRC, kidney renal clear cell carcinoma; KIRP, kidney renal papillary cell carcinoma; LIHC, liver hepatocellular carcinoma; HNSC, head and neck squamous cell carcinoma; LUAD, lung adenocarcinoma; LUSC, lung squamous cell carcinoma; PRAD, prostate adenocarcinoma; STAD, stomach adenocarcinoma; THCA, thyroid carcinoma; UCEC, uterine corpus endometrial carcinoma.

knockdown in A549 cells, confirmed using qPCR (Fig. 7B), significantly inhibited proliferation (P<0.01; Fig. 7C), migration (scratch assay; P<0.001; Fig. 7D and E) and invasion (Transwell assay; P<0.001; Fig. 7F and G).

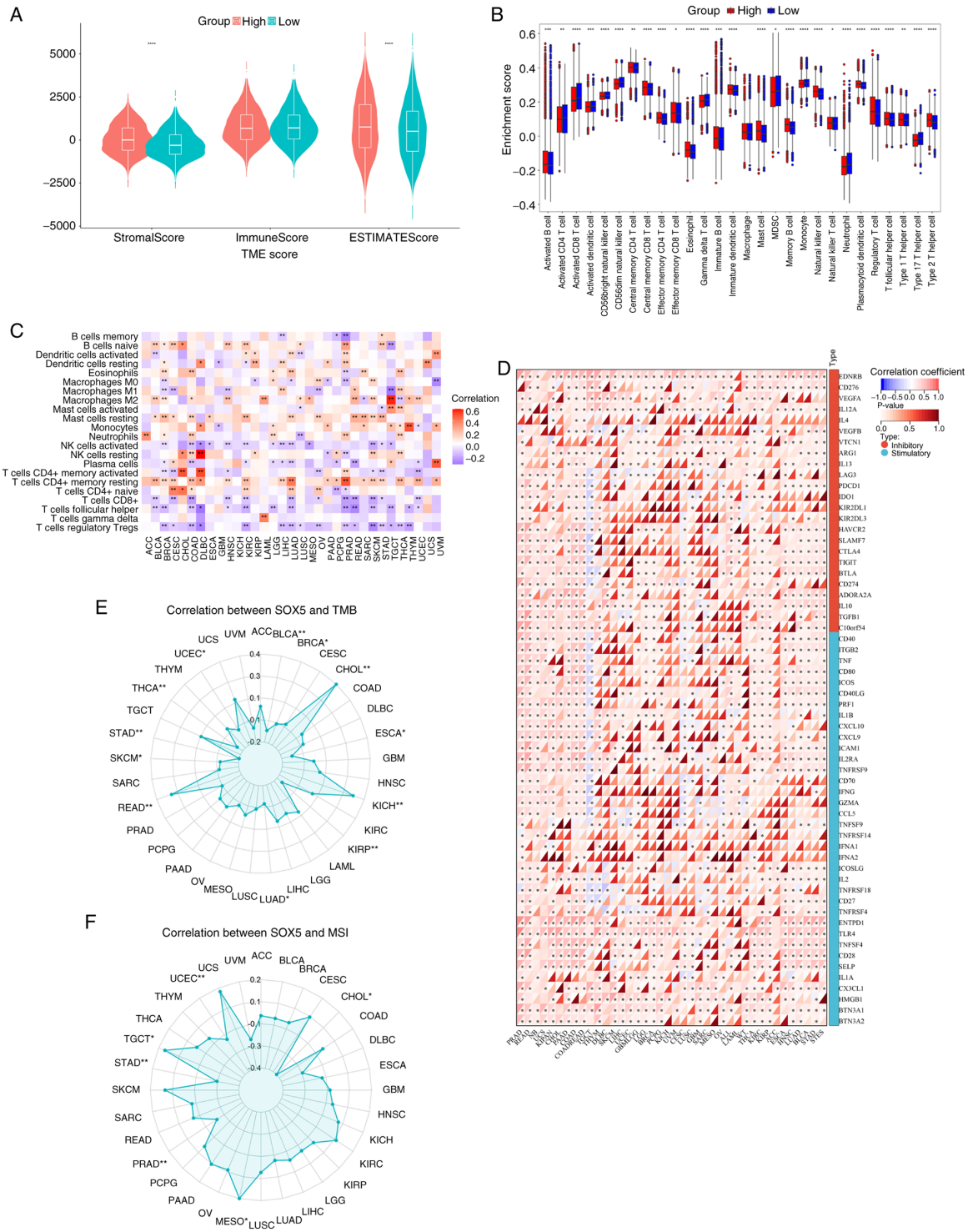

Figure 3. Influence of SOX5 expression on antitumor immunity and immunotherapy response. (A) Correlation between SOX5 and ESTIMATE scores (ESTIMATE Score, Immune Score and Stromal Score). (B) Representative boxplots display the correlation analysis of the cancer-immunity cycle in pan-cancer. The red boxes represent the patients with high levels of SOX5, while blue boxes represent the patients with low levels of SOX5. (C) The relationship between SOX5 expression and tumor-infiltrating immune cells. (D) Pan-cancer association between SOX5 expression and Immune Checkpoint genes.(E) Relationship between SOX5 mRNA expression and TMB. (F) Relationship between SOX5 mRNA expression and MSI. *P<0.05; **P<0.01; ***P<0.001; ****P<0.0001. ns, not significant; SOX5, SRY-related high-mobility group box protein B5; TMB, tumor mutational burden; MSI, microsatellite instability; ESTIMATE, Estimation of Stromal and Immune Cells in Malignant Tumor Tissues Using Expression Data; NK, natural killer; TME, tumor microenvironment.

The study findings are consistent with the established oncogenic role of SOX5 in other cancers. In triple-negative breast cancer, SOX5 drives stemness, EMT and immune evasion (35). In melanoma, SOX5 promotes migration and invasion via transcriptional regulation by the oncogenic long non-coding RNA (lncRNA) SLNCR1 (36). Mechanistically, SOX5 interacts with co-activators, such as transcriptional co-activator with PDZ-binding motif, stabilizing effectors, such as collagen type X α1 chain, and enhancing extracellular matrix remodeling (37,38). In gliomas, SOX5:anaplastic

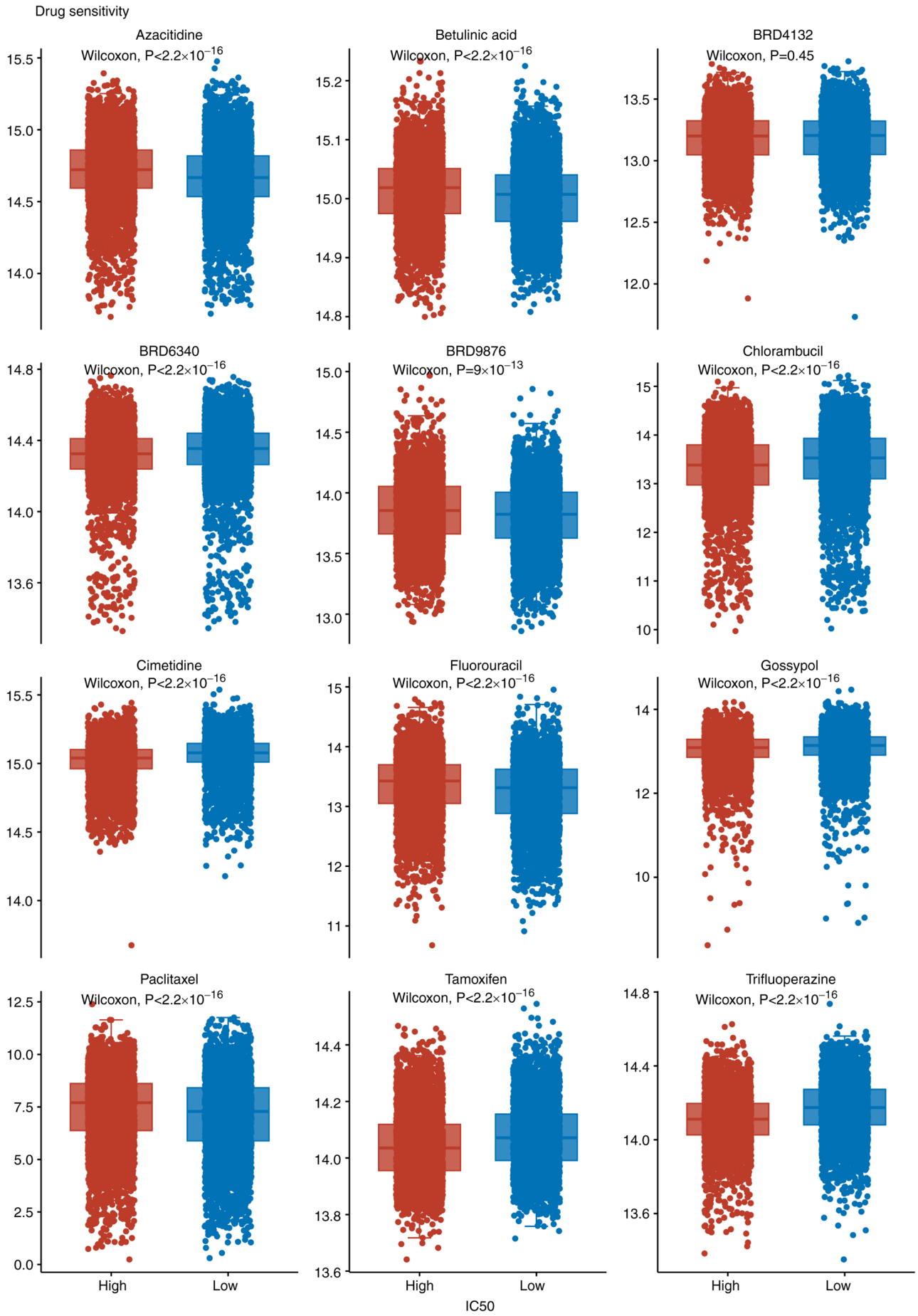

Figure 4. Drug sensitivity analysis. The top 12 SRY-related high-mobility group box protein B5 positively correlated drugs from the Genomics of Drug Sensitivity in Cancer 2 database.

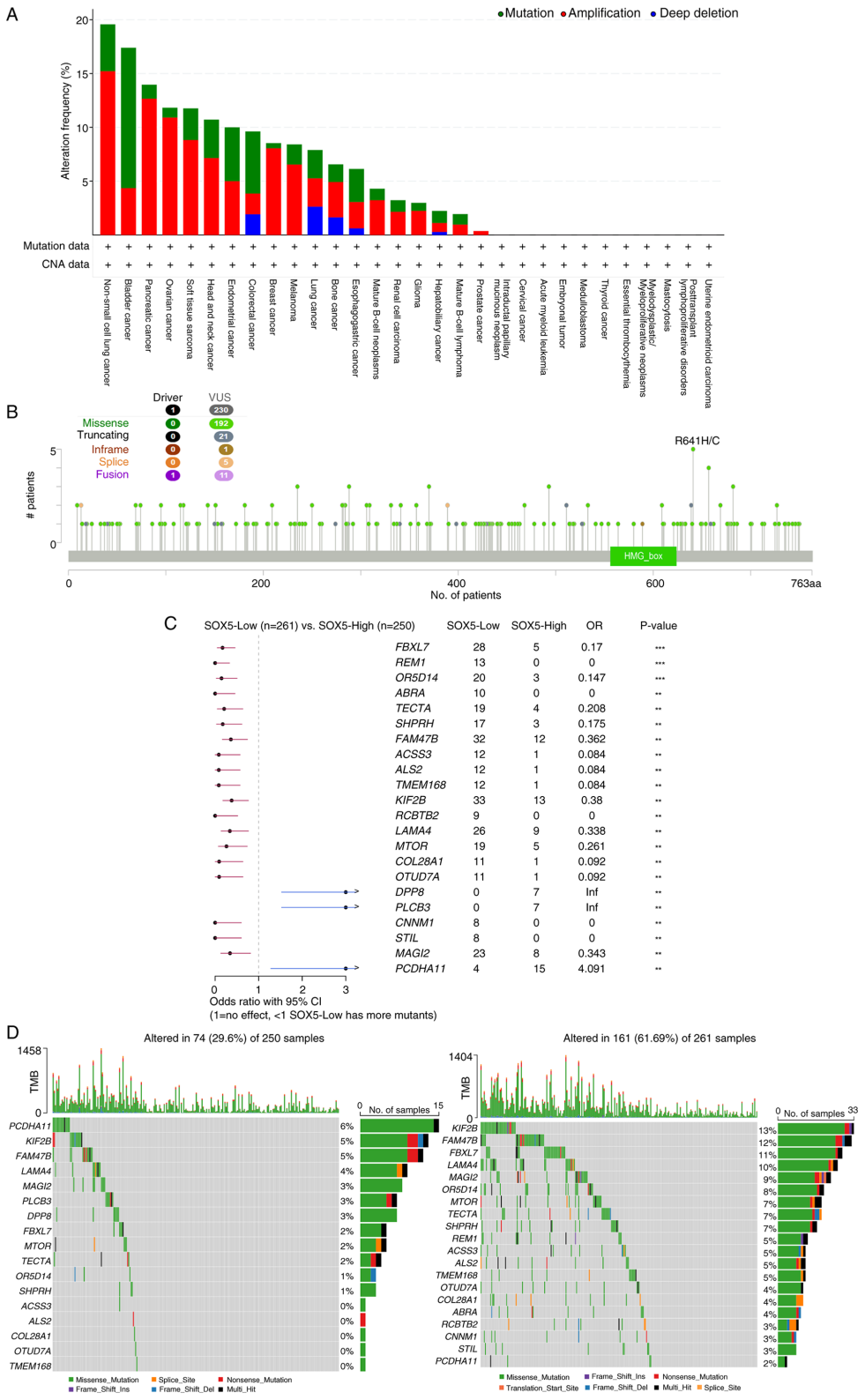

Figure 5. Mutation character of SOX5 in pan-cancer. (A) Alteration frequency of SOX5 in pan-cancer. (B) The subtypes and distributions of SOX5 somatic mutations. (C) Waterfall plots of differential somatic mutations in lung adenocarcinoma, including the $SOX5^{high}$ group and the $SOX5^{low}$ groups. (D) Mutation of SOX5 relation to the mutation of specific signal pathway genes (P<0.05). SOX5, SRY-related high-mobility group box protein B5; OR, odds ratio; CAN, copy number alteration; VUS, variant of uncertain significance; HMG_box, high-mobility group box.

lymphoma kinase (ALK) fusion drives tumor progression, with ALK inhibitors suppressing growth *in vivo* (39). Collectively, these data validate SOX5 as a driver of NSCLC aggressiveness and a potential therapeutic target.

Discussion

Research into the mechanisms driving malignant tumor development and progression has advanced beyond initial

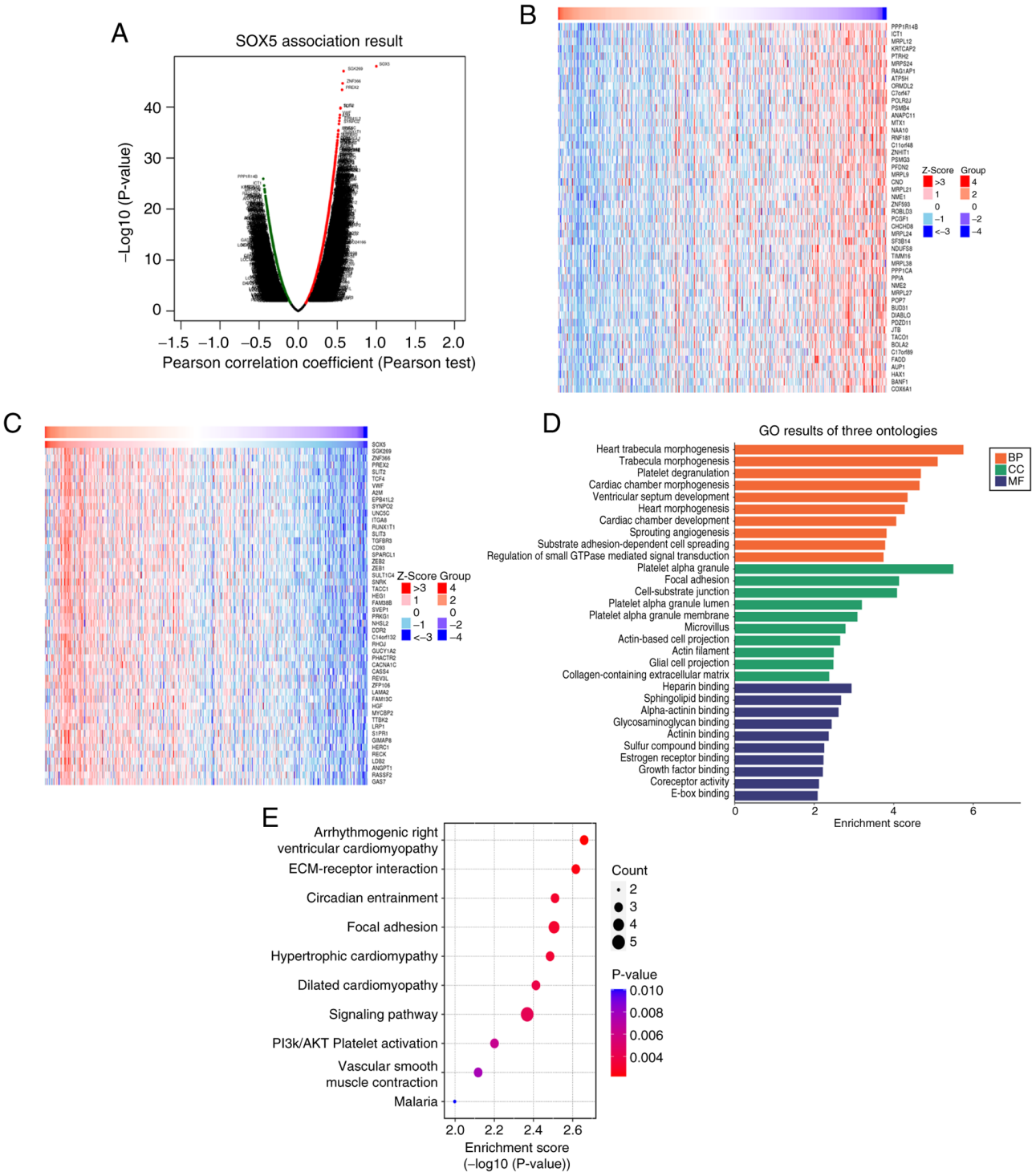

Figure 6. Enrichment analysis of SOX5 co-expression genes in LUAD. (A) The SOX5 co-expression genes in LUAD. (B-C) The top 50 genes were positively and negatively correlated with SOX5. (D) GO and (E) Kyoto Encyclopedia of Genes and Genomes analysis of co-expression genes of SOX5 in the LUAD cohort. SOX5, SRY-related high-mobility group box protein B5; GO, Gene Ontology; LUAD, lung adenocarcinoma; BP, biological process; CC, cellular component; MF, molecular function.

understandings. The rapid development of molecular biological technologies, particularly the application of omics approaches and bioinformatics, has been key in elucidating the functional roles of tumor-associated genes and evaluating their potential as diagnostic biomarkers and therapeutic targets (40-43).

SOX5 displays diverse expression patterns and biological roles across human cancers. In the present study, the role of SOX5 in tumor development was investigated, with a focus on the impact of SOX5 on the TME and its potential mechanisms underlying tumor progression, diagnosis and prognosis, employing a range of bioinformatics tools and statistical approaches.

Results indicate that the functional role of SOX5 in tumorigenesis is highly context-dependent. Dysregulation of SOX5 (upregulation or downregulation) varies notably among cancer

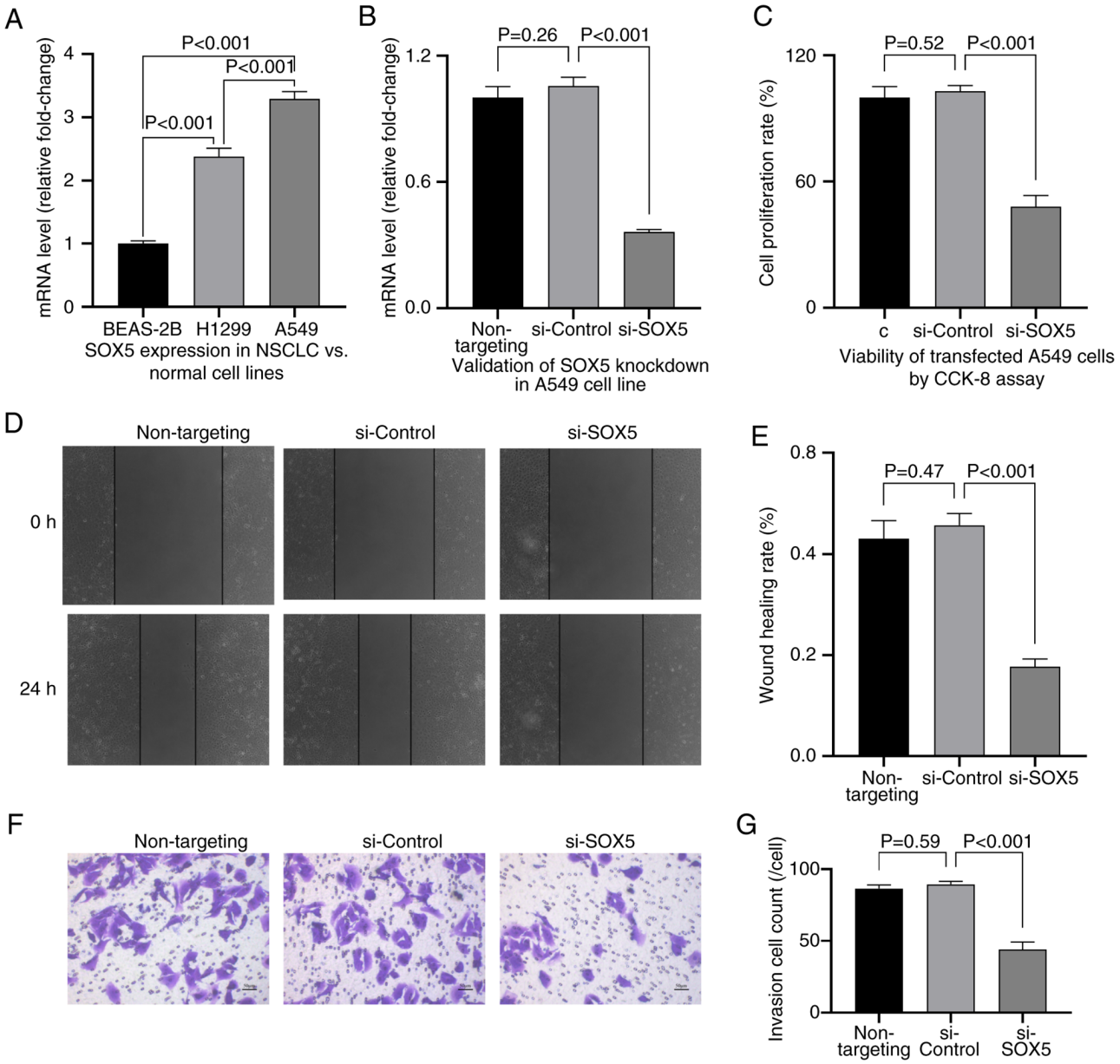

Figure 7. Effect of the SOX5 gene on the biological behavior of non-small cell lung cancer. (A) The expression levels of SOX5 in non-small cell lung cancer cell lines (H1299 and A549) and normal human bronchial epithelial cells (BEAS-2B) were quantified using qPCR. Statistical significance was assessed using a one-way ANOVA followed by Tukey's post hoc test. (B) Validation of SOX5 knockdown in the A549 cell line. The relative mRNA expression level of SOX5 was determined by quantitative PCR in control and SOX5 knockdown groups. Gene expression was calculated using the $2^{-\Delta\Delta Cq}$ method and normalized to GAPDH. Differences among the groups over time were analyzed using a one-way ANOVA followed by Tukey's post hoc test. (C) Cell Counting Kit-8 assay was carried out to assess cell viability in transfected A549 cells. Differences among the groups over time were analyzed using a one-way ANOVA followed by Tukey's post hoc test. (D-E) A wound healing assay was used to assess the migratory abilities of transfected A549 cells. Statistical analysis was performed using a one-way ANOVA followed by Tukey's post hoc test. (F-G) Cell invasion was examined using a Transwell assay in transfected A549 cells. Statistical analysis was performed using a one-way ANOVA followed by Tukey's post hoc test. Data are presented as mean ± SD (n=3). *P<0.05; **P<0.01; ***P<0.001. SOX5, SRY-related high-mobility group box protein B5; qPCR, quantitative PCR; si, small interfering RNA; NC, negative control; pcDNA, plasmid cloning DNA.

types and is strongly influenced by cell-of-origin, driver mutations and the surrounding signaling microenvironment (44-46). Specifically, SOX5 acts predominantly as a tumor suppressor in epithelial carcinomas driven by somatic mutations, where it is frequently downregulated or inactivated (47-49), however exhibits oncogenic properties in specific malignancies such as germ cell tumors, where it is maintained or upregulated (45). This dual role underscores the importance of evaluating SOX5 as a diagnostic or prognostic biomarker and therapeutic target within the context of specific cancer types (45,48,50).

The differential expression of SOX5 across cancers not only reflects its complexity in tumor development but also highlights distinct underlying biological mechanisms (51-53). Reduced SOX5 expression in LUAD, LUSC and BRCA is consistent with a tumor-suppressive role, potentially through regulation of the cell cycle, induction of senescence, or promotion of apoptosis. Conversely, elevated SOX5 expression in germ cell tumors suggests an oncogenic role, possibly by activating pro-proliferative pathways, enhancing migration and invasion or inhibiting apoptosis.

Previous studies further illustrate these divergent roles (3,54,55). In Kaposi's sarcoma, SOX5 overexpression inhibits epithelial-to-mesenchymal transition in Kaposi's sarcoma-associated herpesvirus-infected cells, suggesting a tumor-suppressive function and therapeutic potential. In germ cell tumors, where germ cell-specific expression patterns prevail, increased SOX5 levels may reflect the physiological role it has in reproductive system development, repurposed within the TME to drive uncontrolled growth. This variability in expression patterns underscores the necessity for detailed, cancer type-specific research into SOX5 function. For example, the role of SOX5 in promoting germ cell tumors may involve interactions with specific transcription factors or growth factors that are lost in other types of cancer. In TGCTs, amplification of the 12p11.1-p12.1 region (which contains the SOX5 gene) has been identified as a key event (56), and this 12p gain [including i(12p) and 12p11.2-12.1 amplification] is associated with aggressive tumor progression (55). Although SOX5 is located within this critical region, its expression is lost in some 12p amplification-positive TGCTs, suggesting that its role may be mediated through complex regulatory networks. This mechanism may involve interactions with germ cell tumor-specific signaling pathways such as the KIT/KITLG pathway, or exert effects through regulating cell proliferation, migration and EMT (50).

Beyond its tissue-specific functions, SOX5 shows notable potential as a biomarker. In cancer diagnosis and prognosis, biomarker identification is key to improving patient management and therapeutic efficacy (48,57). The present findings position SOX5 as a promising biomarker with clinical relevance. In LUAD, a high AUC value (0.916) highlights its diagnostic accuracy, suggesting potential utility for early detection. This supports the notion that SOX5 serves a role in early tumor formation and progression, making it a good candidate for early diagnosis, particularly in LUAD, through its expression profiling.

Notable associations between SOX5 expression and survival outcomes, including DSS, DFI and PFI, further reinforce its prognostic value. Variations in SOX5 expression may reflect differences in tumor invasiveness and therapeutic response, thereby impacting patient survival and recurrence risk. In LUAD, low SOX5 expression was associated with worse survival rates, potentially due to its involvement in regulating cell proliferation and apoptosis pathways. Thus, SOX5 expression represents a key prognostic indicator to guide clinical decision-making.

Notably, SOX5 appears to influence the TME, particularly immune evasion mechanisms. The complexity of the TME markedly affects therapeutic outcomes. SOX5 may modulate the immune landscape by regulating immune cell infiltration and related factors, thereby influencing tumor immune surveillance and treatment response (58). The observed positive correlation between elevated SOX5 expression and immune checkpoint levels (PD-L1 and CTLA-4) suggests that SOX5 serves a key immunomodulatory role, potentially facilitating immune evasion within the TME. 'SOX5_High' tumors exhibited activated yet exhausted immune features (including increased immune infiltration, immune scores and TMB, especially in LUAD and UCEC), suggesting SOX5 coordinates both immune recognition and immunosuppressive checkpoint expression.

These findings position SOX5 as a promising predictive biomarker for immune checkpoint blockade (ICB) responsiveness. Patients with high SOX5 expression may benefit more from ICB due to pre-existing checkpoint enrichment. Moreover, targeting SOX5 could enhance ICB efficacy by reducing intrinsic immunosuppression. Future work should aim to validate the mechanistic regulation of immune checkpoints SOX5 may exhibit and associate its expression with clinical ICB outcomes.

Analysis using ESTIMATE and CIBERSORT demonstrated that elevated SOX5 expression is associated with an activated TME and high immune scores, particularly in LUAD and UCEC and is associated with high TMB. SOX5 may regulate the TME through multiple mechanisms, influencing immune cell recruitment, activation and immune escape. Elevated SOX5 could enhance secretion of cytokines and chemokines, recruiting immune cells such as T cells and macrophages. While such infiltration could support antitumor immunity, it may also promote immune escape by recruiting immunosuppressive cells. SOX5 may also regulate immune cell activity by modulating the expression of cell surface molecules such as MHC proteins or immune checkpoint ligands (such as PD-L1), directly affecting T cell activation and inhibition.

The correlation between SOX5 expression and TMB suggests an association with tumor genetic complexity and neoantigen production. As high TMB often predicts improved immunotherapy responses, SOX5 may influence sensitivity to immunotherapy through TMB modulation.

The present study also revealed therapeutic implications of SOX5 expression. Pharmacogenomic analyses showed high SOX5 expression correlates with increased sensitivity to various chemotherapeutics, including azacitidine and betulinic acid. This aligns with the regulation of DNA methyltransferase 1 (DNMT1)/p21 signaling in bladder cancer progression exhibited by SOX5 (48) and suggests that SOX5-overexpressing tumors may be particularly susceptible to DNMT1 inhibitor therapies. Furthermore, targeting the HuR-lncRNA-SOX5 axis, which stabilizes SOX5 transcripts in carcinomas, could exploit this therapeutic vulnerability (59). In addition, SOX5 may sensitize tumor cells to drug-induced apoptosis by regulating cell death pathways, enhancing cell cycle arrest through p53 activation, altering cancer cell metabolism and influencing drug transport and metabolism gene expression (60).

Pan-cancer analysis of SOX5 mutation patterns indicates that alterations in SOX5, particularly in gastric and pancreatic cancers, may drive invasion and therapy resistance. Such mutations could disrupt normal regulatory networks and activate oncogenic pathways (such as Wnt and Notch), contributing to tumor progression. While this may confer resistance to conventional therapies, it offers opportunities for targeted interventions against specific SOX5 alterations.

Although this study provides a comprehensive pan-cancer analysis of SOX5, several important limitations should be acknowledged. First, the research primarily relies on bioinformatic analyses of public databases such as TCGA, and lacks validation in large-scale independent cohorts, which may introduce potential biases or overfitting. For instance, while citation3 developed a prognostic model, it was based solely on TCGA data without involving multi-center samples,

thereby limiting its clinical applicability. Second, functional experiments were confined to *in vitro* cell lines (e.g., A549 and H1299), and lacked *in vivo* animal model validation, which is essential for fully recapitulating the complexity of the tumor microenvironment. Third, the mechanistic insights remain insufficient; for example, the specific pathways through which SOX5 regulates immune infiltration or drug sensitivity were not fully elucidated. Fourth, while the mutation pattern analysis revealed associations between SOX5 alterations and specific signaling pathways, it did not account for tumor heterogeneity and subtype variations, which may affect the generalizability of the findings. Finally, the drug sensitivity data were based on computational predictions and lacked pre-clinical experimental support, necessitating further validation of actual therapeutic efficacy.

In conclusion, the present pan-cancer analysis established SOX5 as a context-dependent regulator with dual roles in tumorigenesis, acting as a tumor suppressor in numerous epithelial cancers while driving oncogenesis in select malignancies. The dysregulation of SOX5 is associated with immune evasion, TME remodeling, genomic instability and patient prognosis. Functional validation demonstrates the role of SOX5 in enhancing proliferation, migration and invasion in NSCLC. These findings position SOX5 as a robust biomarker for cancer diagnosis and prognosis and a promising therapeutic target, offering a strategic avenue for precision oncology across diverse tumor types.

Acknowledgements

Not applicable.

Funding

The present study was supported by the Hunan Natural Science Foundation-Regional Joint Fund (grant no. 2024JJ7601) and Basic Research Guiding Program of Yueyang City Science and Technology Bureau 2024 (20).

Availability of data and materials

The data generated in the present study may be requested from the corresponding author.

Authors' contributions

QY, LO and YT contributed to the conception and design of the study. Data collection was performed by YT, HD, KT, SL, QZ, LY, SB and LL. Formal analysis was conducted by YT, HD, KT, SL, QZ, LY, SB, LL and QY. YT, HD and QY wrote the original draft of the manuscript. The manuscript was reviewed and edited by YT, HD, KT, QZ, LO, QY and SB. LL, SB, LO and QY supervised the study. YT, HD, KT, QZ, SL, LL and QY confirm the authenticity of all the raw data. All authors have read and approved the final version of the manuscript.

Ethics approval and consent to participate

Not applicable.

Patient consent for publication

Not applicable.

Competing interests

The authors declare that they have no competing interests.

References

1. Li Q, Wang W, Yang T, Li D, Huang Y, Bai G and Li Q: LINC00520 up-regulates SOX5 to promote cell proliferation and invasion by miR-4516 in human hepatocellular carcinoma. Biol Chem 403: 665-678, 2022.
2. Wu B, Wang X, Yu R and Xue X: CircWHSC1 serves as a prognostic biomarker and promotes malignant progression of non-small-cell lung cancer via miR-590-5p/SOX5 axis. Environ Toxicol 38: 2440-2449, 2023.
3. Yuan WM, Fan YG, Cui M, Luo T, Wang YE, Shu ZJ, Zhao J, Zheng J and Zeng Y: SOX5 regulates cell proliferation, apoptosis, migration and invasion in KSHV-infected cells. Virol Sin 36: 449-457, 2021.
4. Hu C, Li Q, Xiang L, Luo Y, Li S, An J, Yu X, Zhang G, Chen Y, Wang Y and Wang D: Comprehensive pan-cancer analysis unveils the significant prognostic value and potential role in immune microenvironment modulation of TRIB3. Comput Struct Biotechnol J 23: 234-250, 2023.
5. Yu D, Sun R, Shen D, Ge L, Xue T and Cao Y: Nuclear heme oxygenase-1 improved the hypoxia-mediated dysfunction of blood-spinal cord barrier via the miR-181c-5p/SOX5 signaling pathway. Neuroreport 32: 112-120, 2021.
6. Liang Q, Chu F, Zhang L, Jiang Y, Li L and Wu H: circ-LDLRAD3 knockdown reduces cisplatin chemoresistance and inhibits the development of gastric cancer with cisplatin resistance through miR-588 enrichment-mediated SOX5 inhibition. Gut Liver 17: 389-403, 2023.
7. Sadeghi Z, Dodangeh F and Raheb J: SOX2 overlapping transcript (SOX2-OT) enhances the lung cancer malignancy through interaction with miR-194-5p/SOX5 axis. Iran J Biotechnol 21: e3530, 2023.
8. Tenorio-Castano J, Gómez ÁS, Coronado M, Rodríguez-Martín P, Parra A, Pascual P, Cazalla M, Gallego N, Arias P, Morales AV, *et al*: Lamb-Shaffer syndrome: 20 Spanish patients and literature review expands the view of neurodevelopmental disorders caused by SOX5 haploinsufficiency. Clin Genet 104: 637-647, 2023.
9. Jing Y, Jiang X, Ji Q, Wu Z, Wang W, Liu Z, Guillen-Garcia P, Esteban CR, Reddy P, Horvath S, *et al*: Genome-wide CRISPR activation screening in senescent cells reveals SOX5 as a driver and therapeutic target of rejuvenation. Cell Stem Cell 30: 1452-1471.e10, 2023.
10. Shi L, Zhang H, Sun J, Gao X and Liu C: CircSEC24A promotes IL-1β-induced apoptosis and inflammation in chondrocytes by regulating miR-142-5p/SOX5 axis. Biotechnol Appl Biochem 69: 701-713, 2022.
11. Qiu M, Lu Y, Li J, Gu J, Ji Y, Shao Y, Kong X and Sun W: Interaction of SOX5 with SOX9 promotes warfarin-induced aortic valve interstitial cell calcification by repressing transcriptional activation of LRP6. J Mol Cell Cardiol 162: 81-96, 2022.
12. Chen Z, Shang Y, Zhang X, Duan W, Li J, Zhu L, Ma L, Xiang X, Jia J, Ji X and Gong S: METTL3 mediates SOX5 m6A methylation in bronchial epithelial cells to attenuate Th2 cell differentiation in T2 asthma. Heliyon 10: e28884, 2024.
13. Gu Y, Tang S, Wang Z, Cai L, Lian H, Shen Y and Zhou Y: A pan-cancer analysis of the prognostic and immunological role of β-actin (ACTB) in human cancers. Bioengineered 12: 6166-6185, 2021.
14. Chen R, Zhang C, Cheng Y, Wang S, Lin H and Zhang H: LncRNA UCC promotes epithelial-mesenchymal transition via the miR-143-3p/SOX5 axis in non-small-cell lung cancer. Lab Invest 101: 1153-1165, 2021.
15. Li C, Zhang J and Bi Y: Unveiling the prognostic significance of SOX5 in esophageal squamous cell carcinoma: A comprehensive bioinformatic and experimental analysis. Aging (Albany NY) 15: 7565-7582, 2023.

16. Innella G, Greco D, Carli D, Magini P, Giorgio E, Galesi O, Ferrero GB, Romano C, Brusco A and Graziano C: Clinical spectrum and follow-up in six individuals with Lamb-Shaffer syndrome (SOX5). Am J Med Genet A 185: 608-613, 2021.
17. Edgerley K, Bryson L, Hanington L, Irving R, Joss S, Lampe A, Maystadt I, Osio D, Richardson R, Split M, *et al*: SOX5: Lamb-Shaffer syndrome-A case series further expanding the phenotypic spectrum. Am J Med Genet A 191: 1447-1458, 2023.
18. Leek JT, Johnson WE, Parker HS, Jaffe AE and Storey JD: The sva package for removing batch effects and other unwanted variation in high-throughput experiments. Bioinformatics 28: 882-883, 2012.
19. Rousseaux S, Debernardi A, Jacquiau B, Vitte AL, Vesin A, Nagy-Mignotte H, Moro-Sibilot D, Brichon PY, Lantuejoul S, Hainaut P, *et al*: Ectopic activation of germline and placental genes identifies aggressive metastasis-prone lung cancers. Sci Transl Med 5: 186ra66, 2013.
20. Okayama H, Kohno T, Ishii Y, Shimada Y, Shiraishi K, Iwakawa R, Furuta K, Tsuta K, Shibata T, Yamamoto S, *et al*: Identification of genes upregulated in ALK-positive and EGFR/KRAS/ALK-negative lung adenocarcinomas. Cancer Res 72: 100-111, 2012.
21. Der SD, Sykes J, Pintilie M, Zhu CQ, Strumpf D, Liu N, Jurisica I, Shepherd FA and Tsao MS: Validation of a histology-independent prognostic gene signature for early-stage, non-small-cell lung cancer including stage IA patients. J Thorac Oncol 9: 59-64, 2014.
22. Davis S and Meltzer PS: GEOquery: A bridge between the gene expression omnibus (GEO) and BioConductor. Bioinformatics 23: 1846-1847, 2007.
23. Colaprico A, Silva TC, Olsen C, Garofano L, Cava C, Garolini D, Sabedot TS, Malta TM, Pagnotta SM, Castiglioni I, *et al*: TCGAbiolinks: An R/Bioconductor package for integrative analysis of TCGA data. Nucleic Acids Res 44: e71, 2016.
24. Liao C and Wang X: TCGAplot: An R package for integrative pan-cancer analysis and visualization of TCGA multi-omics data. BMC Bioinformatics 24: 483, 2023.
25. Brune V, Tiacci E, Pfeil I, Döring C, Eckerle S, van Noesel CJ, Klapper W, Falini B, von Heydebreck A, Metzler D, *et al*: Origin and pathogenesis of nodular lymphocyte-predominant Hodgkin lymphoma as revealed by global gene expression analysis. J Exp Med 205: 2251-2268, 2008.
26. Suraokar MB, Nunez MI, Diao L, Chow CW, Kim D, Behrens C, Lin H, Lee S, Raso G, Moran C, *et al*: Expression profiling stratifies mesothelioma tumors and signifies deregulation of spindle checkpoint pathway and microtubule network with therapeutic implications. Ann Oncol 25: 1184-1192, 2014.
27. Robin X, Turck N, Hainard A, Tiberti N, Lisacek F, Sanchez JC and Müller M: pROC: An open-source package for R and S+ to analyze and compare ROC curves. BMC Bioinformatics 12: 77, 2011.
28. Benjamini Y and Hochberg Y: Controlling the False Discovery Rate: A Practical and Powerful Approach to Multiple Testing. J R Statist Soc B 57: 289-300, 1995.
29. Yoshihara K, Shahmoradgoli M, Martínez E, Vegesna R, Kim H, Torres-Garcia W, Treviño V, Shen H, Laird PW, Levine DA, *et al*: Inferring tumour purity and stromal and immune cell admixture from expression data. Nat Commun 4: 2612, 2013.
30. Chen B, Khodadoust MS, Liu CL, Newman AM and Alizadeh AA: Profiling tumor infiltrating immune cells with CIBERSORT. Methods Mol Biol 1711: 243-259, 2018.
31. Hänzelmann S, Castelo R and Guinney J: GSVA: Gene set variation analysis for microarray and RNA-seq data. BMC Bioinformatics 14: 7, 2013.
32. Maeser D, Gruener RF and Huang RS: oncoPredict: An R package for predicting in vivo or cancer patient drug response and biomarkers from cell line screening data. Brief Bioinform 22: bbab260, 2021.
33. Mayakonda A, Lin DC, Assenov Y, Plass C and Koeffler HP: Maftools: Efficient and comprehensive analysis of somatic variants in cancer. Genome Res 28: 1747-1756, 2018.
34. Livak KJ and Schmittgen TD: Analysis of relative gene expression data using real-time quantitative PCR and the 2(-Delta Delta C(T)) Method. Methods 25: 402-408, 2001.
35. Dong G, Wang X, Wang X, Jia Y, Jia Y, Zhao W and Tong Z: Circ_0084653 promotes the tumor progression and immune escape in triple-negative breast cancer via the deubiquitination of MYC and upregulation of SOX5. Int J Biol Macromol 280 (Pt 1): 135655, 2024.
36. Cong L, Zhao Q, Sun H, Zhou Z, Hu Y, Li C, Hao M and Cong X: A novel long non-coding RNA SLNCR1 promotes proliferation, migration, and invasion of melanoma via transcriptionally regulating SOX5. Cell Death Discov 10: 160, 2024.
37. Li Y, Yang S, Qin L and Yang S: TAZ is required for chondrogenesis and skeletal development. Cell Discov 7: 26, 2021.
38. Medina-Menéndez C, Tirado-Melendro P, Li L, Rodríguez-Martín P, Melgarejo-de la Peña E, Díaz-García M, Valdés-Bescós M, López-Sansegundo R and Morales AV: Sox5 controls the establishment of quiescence in neural stem cells during postnatal development. PLoS Biol 23: e3002654, 2025.
39. Tsai CC, Huang MH, Fang CL, Hsieh KL, Hsieh TH, Ho WL, Chang H, Tsai ML, Kao YC, Miser JS, *et al*: An infant-type hemispheric glioma with SOX5::ALK: A novel fusion. J Natl Compr Canc Netw 22: e237102, 2024.
40. Sara H, Kallioniemi O and Nees M: A decade of cancer gene profiling: From molecular portraits to molecular function. Methods Mol Biol 576: 61-87, 2010.
41. Legge F, Ferrandina G and Scambia G: From bio-molecular and technology innovations to clinical practice: Focus on ovarian cancer. Ann Oncol 17 (Suppl 7): vii46-vii48, 2006.
42. Lu DY, Qu RX, Lu TR and Wu HY: Cancer bioinformatics for updating anticancer drug developments and personalized therapeutics. Rev Recent Clin Trials 12: 101-110, 2017.
43. Shi Y, Wang Y, Zhang W, Niu K, Mao X, Feng K and Zhang Y: N6-methyladenosine with immune infiltration and PD-L1 in hepatocellular carcinoma: Novel perspective to personalized diagnosis and treatment. Front Endocrinol (Lausanne) 14: 1153802, 2023.
44. Chen X, Fu Y, Xu H, Teng P, Xie Q, Zhang Y, Yan C, Xu Y, Li C, Zhou J, *et al*: SOX5 predicts poor prognosis in lung adenocarcinoma and promotes tumor metastasis through epithelial-mesenchymal transition. Oncotarget 9: 10891-10904, 2017.
45. Ueda R, Yoshida K, Kawase T, Kawakami Y and Toda M: Preferential expression and frequent IgG responses of a tumor antigen, SOX5, in glioma patients. Int J Cancer 120: 1704-1711, 2007.
46. Chen M, Zou S, He C, Zhou J, Li S, Shen M, Cheng R, Wang D, Zou T, Yan X, *et al*: Transactivation of SOX5 by Brachyury promotes breast cancer bone metastasis. Carcinogenesis 41: 551-560, 2020.
47. Yang B, Zhang W, Sun D, Wei X, Ding Y, Ma Y and Wang Z: Downregulation of miR-139-5p promotes prostate cancer progression through regulation of SOX5. Biomed Pharmacother 109: 2128-2135, 2019.
48. Wu L, Yang Z, Dai G, Fan B, Yuan J, Liu Y, Liu P and Ou Z: SOX5 promotes cell growth and migration through modulating the DNMT1/p21 pathway in bladder cancer. Acta Biochim Biophys Sin (Shanghai) 54: 987-998, 2022.
49. Pei XH, Lv XQ and Li HX: SOX5 induces epithelial to mesenchymal transition by transactivation of Twist1. Biochem Biophys Res Commun 46: 322-327, 2014.
50. Xue JD, Xiang WF, Cai MQ and Lv XY: Biological functions and therapeutic potential of SRY related high mobility group box 5 in human cancer. Front Oncol 14: 1332148, 2024.
51. Docherty AR, Mullins N, Ashley-Koch AE, Qin X, Coleman JRI, Shabalin A, Kang J, Murnyak B, Wendt F, Adams M, *et al*: GWAS meta-analysis of suicide attempt: identification of 12 genome-wide significant loci and implication of genetic risks for specific health factors. Am J Psychiatry 180: 723-738, 2023.
52. Vinyals A, Ferreres JR, Calbet-Llopart N, Ramos R, Tell-Martí G, Carrera C, Marcoval J, Puig S, Malvehy J, Puig-Butillé JA and Fabra À: Oncogenic properties via MAPK signaling of the SOX5-RAF1 fusion gene identified in a wild-type NRAS/BRAF giant congenital nevus. Pigment Cell Melanoma Res 35: 450-460, 2022.
53. Collins FL, Roelofs AJ, Symons RA, Kania K, Campbell E, Collie-Duguid ESR, Riemen AHK, Clark SM and De Bari C: Taxonomy of fibroblasts and progenitors in the synovial joint at single-cell resolution. Ann Rheum Dis 82: 428-437, 2023.
54. Sridharan S and Basu A: Distinct roles of mTOR targets S6K1 and S6K2 in breast cancer. Int J Mol Sc 21: 1199, 2020.
55. Blanco L and Tirado CA: Testicular germ cell tumors: A cytogenomic update. J Assoc Genet Technol 44: 128-133, 2018.
56. Mostert MC, Verkerk AJ, van de Pol M, Heighway J, Marynen P, Rosenberg C, van Kessel AG, van Echten J, de Jong B, Oosterhuis JW and Looijenga LH: Identification of the critical region of 12p over-representation in testicular germ cell tumors of adolescents and adults. Oncogene 16: 2617-2627, 1998.

57. Cai Y and Jia Y: Circular RNA SOX5 promotes the proliferation and inhibits the apoptosis of the hepatocellular carcinoma cells by targeting miR-502-5p/synoviolin 1 axis. Bioengineered 13: 3362-3370, 2022.
58. Knights AJ, Farrell EC, Ellis OM, Lammlin L, Junginger LM, Rzeczycki PM, Bergman RF, Pervez R, Cruz M, Knight E, *et al*: Synovial fibroblasts assume distinct functional identities and secrete R-spondin 2 in osteoarthritis. Ann Rheum Dis 82: 272-282, 2023.
59. Wang L, Ye S, Wang J, Gu Z, Zhang Y, Zhang C and Ma X: HuR stabilizes lnc-SOX5 mRNA to promote tongue carcinogenesis. Biochemistry (Mosc) 82: 438-445, 2017.
60. Li QS, Shabalin AA, DiBlasi E, Gopal S, Canuso CM; FinnGen, International Suicide Genetics Consortium; Palotie A, Drevets WC, Docherty AR and Coon H: Genome-wide association study meta-analysis of suicide death and suicidal behavior. Mol Psychiatry 28: 891-900, 2023.

Copyright © 2025 Tong et al. This work is licensed under a Creative Commons Attribution-NonCommercial-NoDerivatives 4.0 International (CC BY-NC-ND 4.0) License.